Expanded View Figures

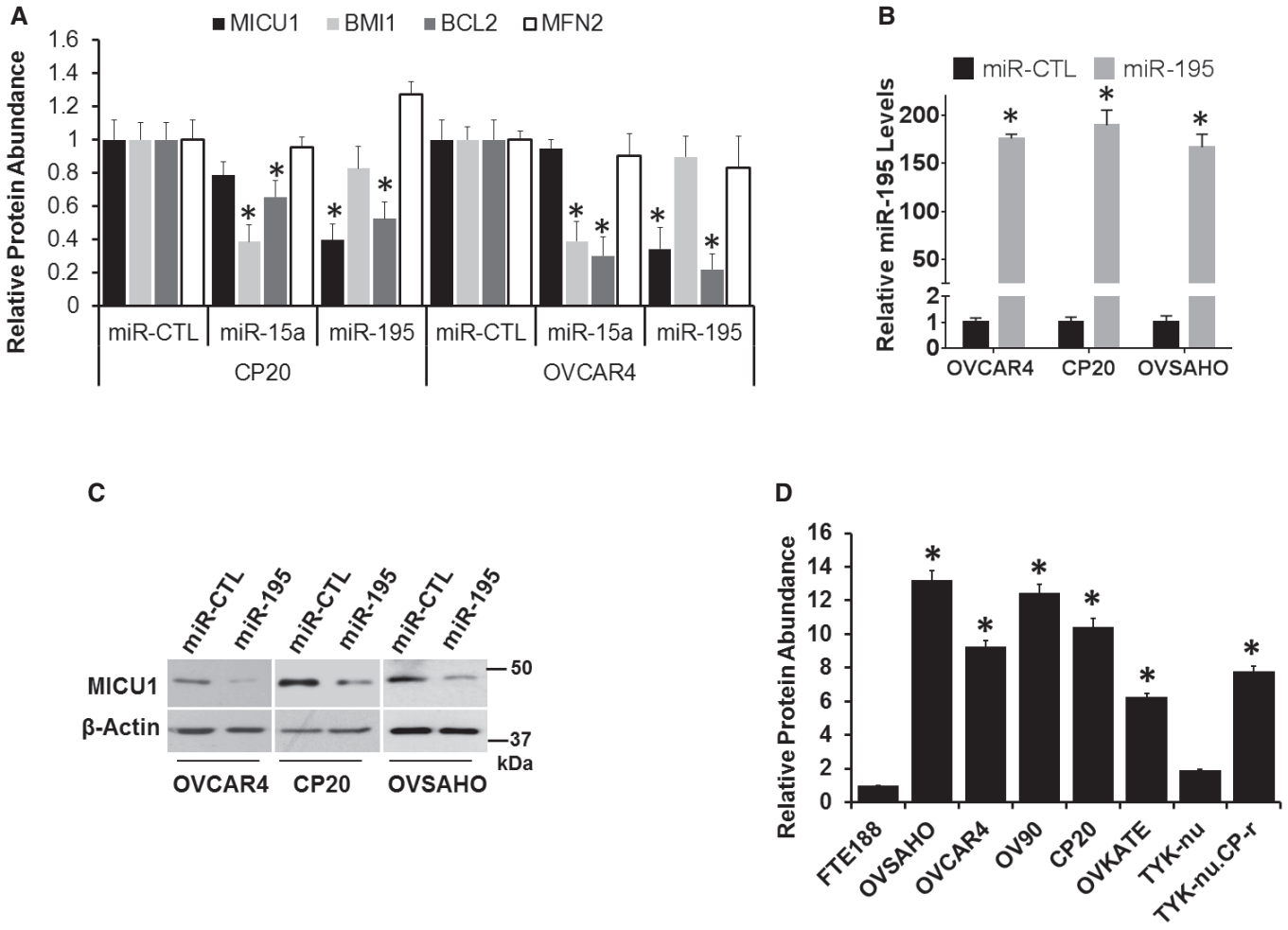

Figure EV1. miR-195 regulates MICU1 expression.

A Graph showing densitometric quantification of Western blot bands for CP20 and OVCAR4 cells in Fig 1A (n = 3, biological repeats mean ± SE) normalized with GAPDH. *P < 0.05, Student's t-test.

B Ovarian cancer cells were transfected with either non-target microRNA (miR-CTL) or miR-195. Total RNA was isolated and miR-195 levels normalized with U6 were plotted. Data are mean ± SD, n = 3 biological repeats, *P < 0.05, Student's t-test.

C MICU1 expression in cells transfected with miR-CTL and miR-195. β-Actin was used as the loading control.

D Graph showing densitometric quantification of Western blot bands for ovarian cancer cells in Fig 1C. Values are represented as mean fold change ± SD, n = 3 biological repeats, *P < 0.05, Student's t-test.

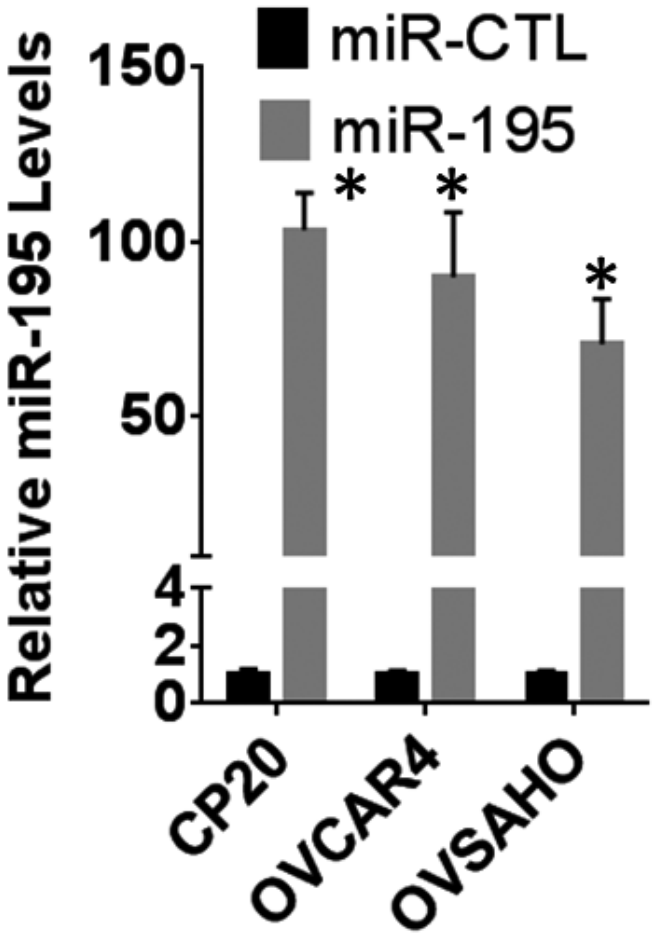

Figure EV2. Quantitation of microRNA expression.
Ovarian cancer cells were transfected with either non-target microRNA (miR-CTL) or miR-195. Total RNA was isolated and miR-195 levels normalized with U6 were plotted. Data are mean ± SD, $n = 3$ biological repeats, $^*P < 0.05$, Student's *t*-test.

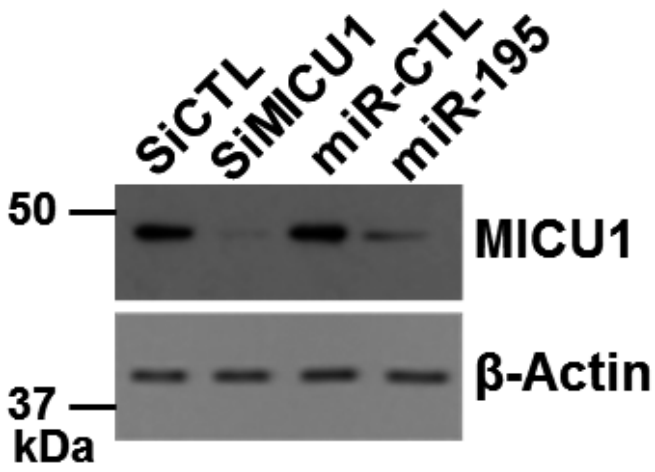

Figure EV3. Efficacy of MICU1 inhibition by miR-195 and siRNA.
After siRNA and miR transfection as shown in the image, efficacy of MICU1 inhibition was evaluated using immunoblotting. Similarly, transfected cells were used to evaluate $[Ca^{2+}]_{out}$ shown in Fig 3. β-Actin was used as loading control.

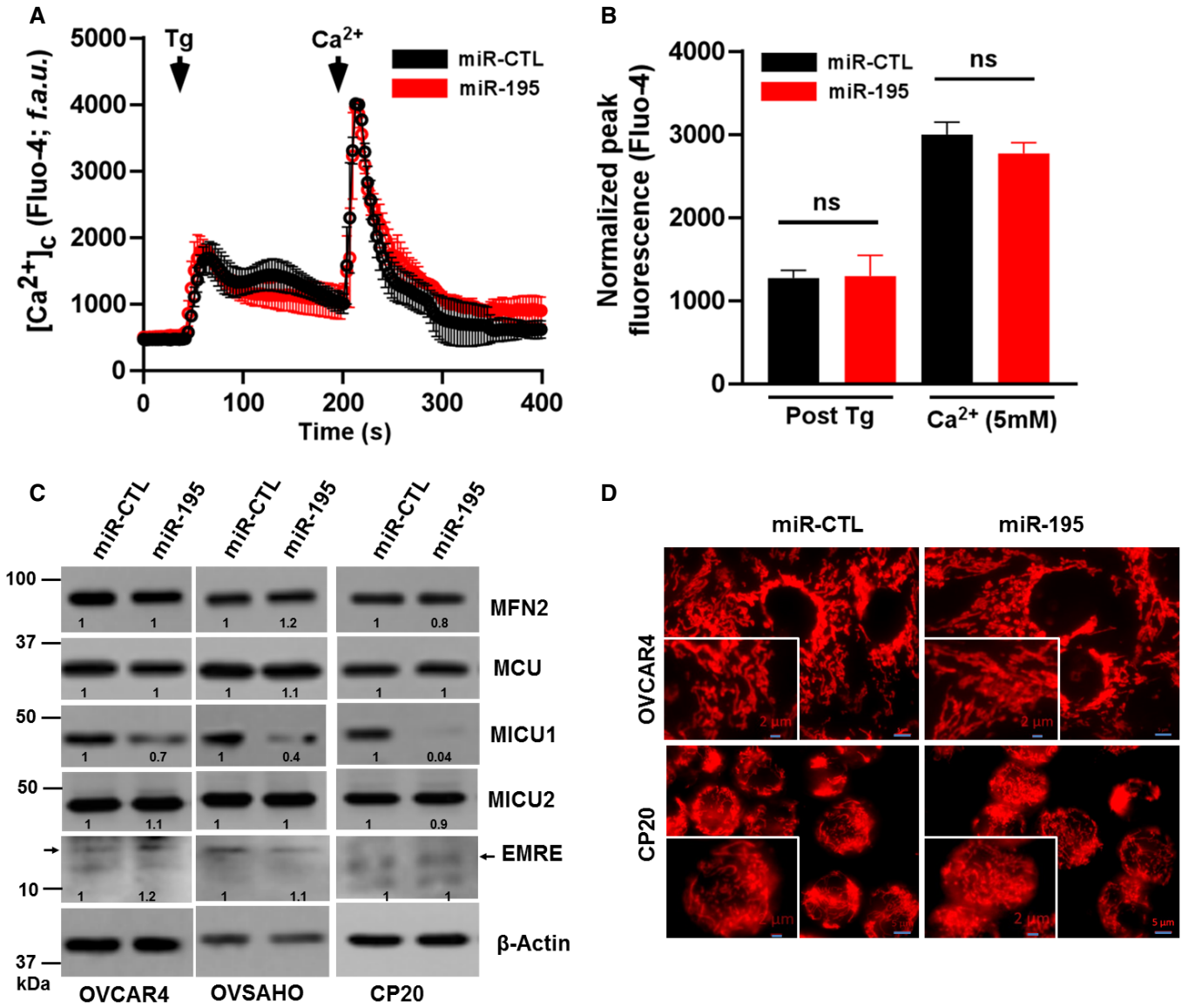

Figure EV4. miR-195 overexpression does not alter cytosolic Ca^{2+}, MCU complex protein expression, and mitochondrial morphology in ovarian cancer.

A, B After miR-CTL or miR-195 transfection in CP20 cells cytosolic Ca^{2+} was measured (A) Fluorescence traces (Fluo-4 AM) vs time (s) showing Tg (4 µM) induced characteristic increase in cytosolic Ca^{2+} (5 mM) and uptake and retention of SOC activity following Ca^{2+} addition in both miR-CTL and miR 195 transfected cells. Tg and Ca^{2+} were added as indicated. (B) Quantification of normalized peak fluorescence (Fluo-4 AM) after Tg stimulation and Ca^{2+} addition. Non-parametric *t*-test determined the level of significance of fluorescence between miR-CTL and miR-195-treated cells (n = 3, biological repeats), (ns = not significant, Student's *t*-test).

C After miR-CTL or miR-195 transfection in OVCAR4, OVSAHO, and CP20 cells, cell lysate was evaluated for the expression of MFN2, MCU, MICU1, MICU2, and EMRE. β-Actin is used as loading control.

D Immunofluorescence of CP20 and OVCAR4 cells labeled with Mitotracker red (Scale bar 5 µM), inset shows enlarged image portion (Scale bar 2 µM).

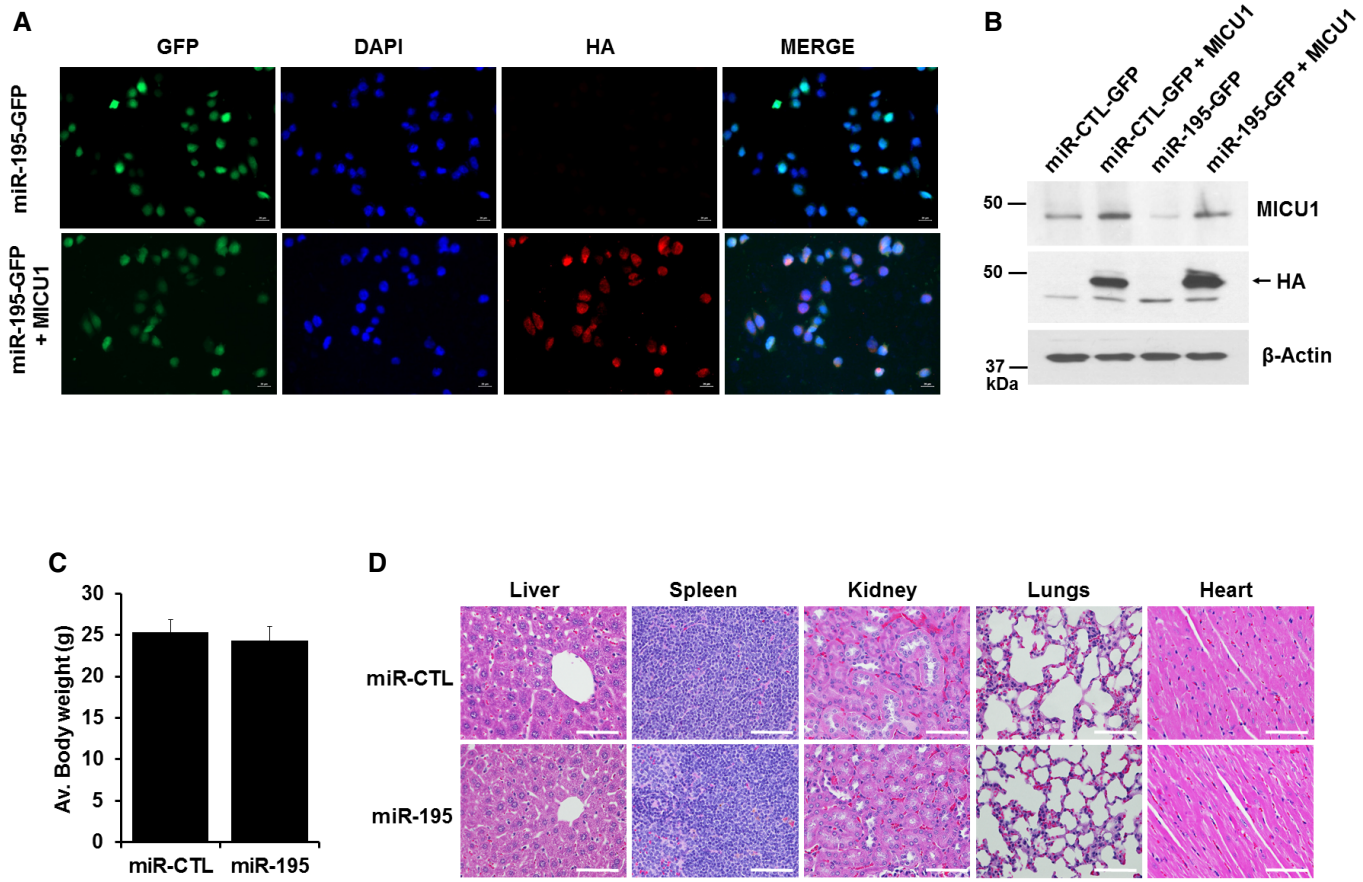

Figure EV5. MICU1 stable cell line and toxicity assessment in miR-CTL and miR-195 tumor model.

A, B MICU1 was stably expressed in miR stable transfected CP20 cells by using pLenti-C-HA-IRES-BSD plasmid (OriGene Technologies); MICU1 stable cells were selected using Blasticidin. MICU1 expression in stable cells is shown by IFC (A) and immunoblotting (B).

C, D Toxicity in experimental mice caused by miR-195 overexpressing CP20 cells was assessed by changes in body weight and histology of vital organs. (C) Average body weight of mice from miR-CTL and miR-195 experimental groups immediately before euthanasia. Mean ± SD, n = 10 is shown. (D) Representative H&E-stained sections of tissues (liver, spleen, kidneys, lungs, and heart) from miR-CTL and miR-195 mice visualized using an upright epi-fluorescent microscope (Nikon NI-U, Plan Apochromatic). Scale bar 25 μM.